



HAL
open science

Temperature- and pressure-dependence of the hydrogen bond network in plastic ice VII

Alberto Toffano, John Russo, Maria Rescigno, Umbertoluca Ranieri, Livia E Bove, Fausto Martelli

► **To cite this version:**

Alberto Toffano, John Russo, Maria Rescigno, Umbertoluca Ranieri, Livia E Bove, et al.. Temperature- and pressure-dependence of the hydrogen bond network in plastic ice VII. *Journal of Chemical Physics*, 2022, 157 (9), pp.094502. 10.1063/5.0111189 . hal-03874995

HAL Id: hal-03874995

<https://hal.science/hal-03874995>

Submitted on 28 Nov 2022

HAL is a multi-disciplinary open access archive for the deposit and dissemination of scientific research documents, whether they are published or not. The documents may come from teaching and research institutions in France or abroad, or from public or private research centers.

L'archive ouverte pluridisciplinaire **HAL**, est destinée au dépôt et à la diffusion de documents scientifiques de niveau recherche, publiés ou non, émanant des établissements d'enseignement et de recherche français ou étrangers, des laboratoires publics ou privés.

Temperature- and pressure-dependence of the hydrogen bond network in plastic ice VII

Accepted Manuscript: This article has been accepted for publication and undergone full peer review but has not been through the copyediting, typesetting, pagination, and proofreading process, which may lead to differences between this version and the Version of Record.

Cite as: J. Chem. Phys. (in press) (2022); <https://doi.org/10.1063/5.0111189>

Submitted: 18 July 2022 • Accepted: 09 August 2022 • Accepted Manuscript Online: 09 August 2022

Alberto Toffano, John Russo,  Maria Rescigno, et al.



View Online



Export Citation



CrossMark

ARTICLES YOU MAY BE INTERESTED IN

[A programmable magnetoelastic sensor array for self-powered human-machine interface](#)
Applied Physics Reviews **9**, 031404 (2022); <https://doi.org/10.1063/5.0094289>

(); <https://doi.org/10.1063/PT.6.1.20220809a>

[Accuracy of approximate methods for the calculation of absorption-type linear spectra with a complex system-bath coupling](#)

The Journal of Chemical Physics (2022); <https://doi.org/10.1063/5.0100977>

Lock-in Amplifiers
up to 600 MHz



Zurich
Instruments



J. Chem. Phys. (in press) (2022); <https://doi.org/10.1063/5.0111189>

© 2022 Author(s).

Temperature- and pressure-dependence of the hydrogen bond network in plastic ice VII

Alberto Toffano,^{1,2} John Russo,³ Maria Rescigno,³ Umbertolucà Ranieri,³ Livia E. Bove,^{4,3,5} and Fausto Martelli^{2, a)}

¹⁾*School of Mathematics, University of Bristol, Bristol BS8 1TW, United Kingdom*

²⁾*IBM Research Europe, Hartree Centre, Daresbury, WA4 4AD, United Kingdom*

³⁾*Department of Physics, Sapienza University of Rome, Piazzale Aldo Moro 5, 00185 Rome, Italy*

⁴⁾*Institut de Minéralogie, de Physique des Matériaux et de Cosmochimie, Sorbonne Université, CNRS UMR7590, 75005 Paris, France*

⁵⁾*Earth and Planetary Science Laboratory, Institute of Physics, Ecole Polytechnique Fédérale de Lausanne, CH-1015 Lausanne, Switzerland*

We model, via classical molecular dynamics simulations, the plastic phase of ice VII across a wide range of the phase diagram of interest for planetary investigations. Although structural and dynamical properties of plastic ice VII are mostly independent on the thermodynamic conditions, the hydrogen bond network (HBN) acquires a diverse spectrum of topologies distinctly different from that of liquid water and of ice VII simulated at the same pressure. We observe that the HBN topology of plastic ice carries some degree of similarity with the crystal phase, stronger at thermodynamic conditions proximal to ice VII, and gradually lessening upon approaching the liquid state. Our results enrich our understanding of the properties of water at high pressure and high temperature, and may help in rationalizing the geology of water-rich planets.

I. INTRODUCTION

With at least nineteen solid forms, water has the most complex phase diagram of any pure substance.^{1,2} At high pressures and high temperatures, water is of interest for the Earth's mantle and for the geology of water-rich planets³⁻⁹. At these conditions, water can acquire several high density forms^{1,8,10-22}, one of which is ice VII,^{8,20,21}. Oxygen atoms in ice VII form a body-centered cubic (bcc) structure with $Pn\bar{3}m$ space group and two atoms per unit cell. Each oxygen atom is surrounded by four hydrogen atoms, two of which covalently bonded and two H-bonded to it, according to the Bernal-Fowler rules²³. The hydrogen bond network (HBN) is endowed with proton disorder and consists of two independent interpenetrating sub-networks not hydrogen bonded to each other, each of them topologically equivalent to the HBN of cubic ice^{17,24}. Proton disorder disappears at low temperatures, when ice VII transitions to proton-ordered ice VIII²⁵⁻²⁷. The domain of stability of ice VII extends above 2 GPa across a wide region of pressures and temperatures (fig. 1). Such large domain of stability renders it extremely interesting for the modeling of the interior of icy moons where it is a stable form, and for planetary investigations. In particular, it is believed that the thermoelastic properties of ice VII (as well as of other high-pressure polymorphs) can have implications for the dynamics of cold slab subduction in the Earth lower mantle, and for the evolution of icy planets and satellites. Ice VII is able to dissolve several halides^{20,21,28,29}, and recent first-principle simulations have shown that, upon breaking the HBN of ice VII, salt impurities are able to

diffuse within the ice VII matrix causing proton diffusion. As a result, ice VII may allow the release of nutrients from the core of super-Earths and mini-Neptunes to liquid oceans³⁰, hence affecting their compositions. As a matter of fact, several "phases" of ice VII seem to exist. According to *ab initio* molecular dynamics simulations, continuous electric fields can allow protons to jump from one molecule to another following a Grotthuss-like mechanism, effectively generating superionic ice VII³¹. Superionic phases of other ice polymorphs can be obtained at higher pressures and temperatures and have been deemed to be of relevance to giant icy bodies like Uranus and Neptune^{7,16,32-34}. Numerical simulations place superionic ice VII at the boundaries of ice VII and liquid water above 20 GPa and 2000 K^{32,35-37}. Nonetheless, both classical and *ab initio* simulations have predicted that, at lower pressure and temperature, the boundary between ice VII and liquid water is a plastic phase^{32,37-48} (fig. 1). At these conditions, oxygen atoms remain crystallographically ordered, but water molecules rotate on time scales comparable to those in the liquid state creating a dynamical HBN. This effect arises as a combination of the temperature and pressure exerted to ice VII resulting in enough energy to break HBs, but not enough to melt the sample nor to allow hydrogen atoms to detach from the oxygens. As a consequence, ice VII and its plastic counterparts are separated by a first-order phase transition^{32,40}. All these phases, namely crystalline, plastic and superionic ice VII, reflect the tremendous (and intriguing) complexity of this crystallographic phase and of high pressure water at large.

Computer simulations have widely investigated the structural and dynamical properties of plastic ices³⁷⁻⁴⁸, but no focus has been devoted to the HBN and its topology. Considering the relevance of high pressure crystalline phases endowed with hydrogen mobility in ex-

^{a)}Electronic mail: fausto.martelli@ibm.com

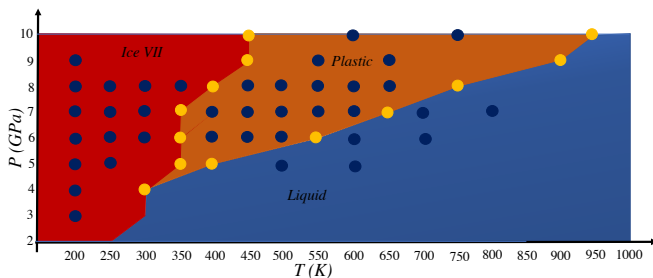


FIG. 1. Pictorial representation of the pressure Vs temperature phase diagram obtained from our simulations. The yellow circles represent the thermodynamic points simulated to locate the existence domain of the plastic phase. The blue circles represent the thermodynamic points adopted to perform our investigations.

plaining the properties of water-rich (exo)planets and the potential role of these phases in transferring salts to liquid oceans via modifications of the HBN, rationalizing the properties of the HBN of plastic ice VII may be of relevance for planetary science. In this article, we inspect the topology of the HBN of plastic ice VII modeled via classical molecular dynamics simulations at different thermodynamic conditions. We limit our investigations to $P \leq 10$ GPa, above which proton diffusion (not captured by classical molecular dynamics) might occur. We show that, although structural and dynamical properties are mostly independent on the thermodynamic condition, the HBN acquires distinct topologies. In fig. 1 we report a schematic representation of the phase diagram obtained from our simulations. The blue circles represent the thermodynamic points at which we have inspected the topology of the HBN.

The article is organized as follows: in Section II we describe the numerical setup and the analysis adopted to inspect the HBN. Section III is devoted to the discussion of the results of our work, and in Section IV we present our conclusions.

II. NUMERICAL SIMULATIONS

A. Classical molecular dynamics simulations

Our study is based on classical molecular dynamics (MD) simulations of a system composed of $N = 1024$ rigid water molecules described by the TIP4P/2005 interaction potential⁴⁹ in the isobaric (NPT) ensemble. This water model is able to reproduce relatively well the phase diagram of water at the thermodynamic conditions of interest of this work^{40,50}. Numerical simulations have been performed with the GROMACS 18.0.1 package⁵¹. Coulombic and Lennard-Jones interactions are calculated with a cutoff distance of 1.1 nm and long-range electrostatic interactions are treated using the Particle-Mesh Ewald (PME) algorithm. Temperatures

and pressures are controlled using the Nosé-Hoover thermostat^{52,53} with a constant of 1 ps, and the Parrinello-Rahman barostat⁵⁴ with a time constant of 1 ps. Equations of motions are integrated with the Verlet algorithm⁵⁵ with a time step of 2 fs. After initial equilibrations of 1 ns, we perform production runs for another 2 ns. The initial configurations of ice VII have been obtained with the GenIce tool⁵⁶

B. Analysis of the hydrogen bond network

We investigate the topology of the HBN using the ring statistics, a theoretical tool that has been instrumental in understanding the properties of water^{10,57–65}, water systems^{66–72} and network-forming materials^{73–81}.

In order to compute the ring statistics it is necessary to (i) define the link between atoms/molecules, (ii) provide a definition of ring, or closed loop, and (iii) provide a criterion to count rings. Possible definitions of link between molecules can be based, e.g., on the formation of bonds, interaction energies, geometric distances, etc.. We follow the geometrical criterion of HB reported in Ref.⁸² according to which two water molecules A and B are hydrogen bonded if the distance $d_{O_A O_B} < 3.5$ Å and the angle $H_B \widehat{O_B} O_A < 30^\circ$. In this regard, any quantitative measure of HBs in liquid water is somewhat ambiguous, since the notion of an HB itself is not uniquely defined. However, qualitative agreement between many proposed definitions have been deemed satisfactory over a wide range of thermodynamic conditions^{83,84}. Next, we define as ring any close loop that, starting from a water molecule and recursively traversing the network defined by HBs, ends when the starting point is reached or the path is shorter than the maximal size considered (18 water molecules in our case)⁵⁹. Although several methodologies and criteria have been introduced to investigate the network topology in network-forming materials, the methodology adopted in this work provides information about the HBN directly linked to translational diffusion, rotational dynamics and structural properties of water⁵⁸.

III. RESULTS

To locate the domain of existence of the plastic phase reported in fig. 1, we have followed previous investigations and combined information about the radial distribution function computed between oxygen atoms, $g_{OO}(r)$, the mean square displacement of oxygen atoms, the rotational autocorrelation function evaluated on the intramolecular O-H bonds, and the angular distribution of the polar angles θ for the O-H vectors^{37–48}. In this article, we will not discuss them, rather we will focus on the HBN, reported in fig. 2.

The HBN of ice VII is rich in hexagonal rings $n = 6$, as reported in fig. 2 (a). The hexagonal geometry dominates the network, accounting for $\sim 40\%$ of the configurations.

Longer rings ($n > 6$) occur only on even lengths, namely $n = 8, n = 10, n = 12, n = 14, n = 16$ and $n = 18$, each present in variable percentage fluctuating around $\sim 10\%$. The lack of odd rings is due to the fact that ice VII has two interpenetrating and independent cubic networks. As expected, the topology of the HBN is mostly independent on the pressure in ice VII. Increasing the pressure from 6 GPa (black circles) to 7 GPa (red squares) does not cause any sensitive effect in the rings pathways. Fig. 3 a) shows a representative snapshot of the network of ice VII emphasizing an hexagonal (green) and an octagonal (orange) ring. In fig. 2 (b) and (c) we report the $P(n)$ computed on isobars at $P = 6$ GPa and $P = 7$ GPa, respectively (our results apply also to other pressures). At a given pressure, depending on the temperature, the plastic phase carries a certain degree of reminiscence of the HBN of ice VII. Such similarity is stronger at thermodynamic conditions closer to ice VII and tends to lessen upon moving towards the liquid at higher temperatures. At $P = 6$ GPa and $T = 400$ K (panel (b), red squares) the system is plastic (see fig. 1) and water molecules are allowed to rotate. As a consequence, the configurational entropy increases with respect to ice VII. The topology of the HBN is therefore different from that of ice VII in the sense that accounts for odd rings and reaches sizes up to $n = 15$. On the other hand, it is possible to notice that the $P(n)$ does not follow a smooth distribution like in the liquid at the same pressure (orange symbols) but, rather, is characterized by an alternating profile of local maxima in correspondence with $n = 4, n = 6$ and $n = 8$ and corresponding local minima at $n = 5$ and $n = 7$. Upon further increasing the temperature to $T = 450$ K (green diamonds) and to $T = 500$ K (blue triangles) we observe a progressive smoothing $P(n)$ with a slight decrease of $n = 8$ and a corresponding slight increase of $n = 5$ which, nonetheless, still represents a minimum at all thermodynamic conditions. Considering that pentagonal and heptagonal rings are not present in ice VII, the minimum in correspondence of $n = 5$ for the plastic phases is a further indication of the link with ice VII. The minima at $n = 5$ and $n = 7$ eventually disappears in the liquid phase (orange symbols), whose topology is very broad and dominated by $n = [5, 11]$, with long rings accounting for the high density of the liquid phase. The trend that emerges, therefore, clearly shows how the HBN of plastic ice VII lean towards that of liquid water upon increasing the temperature at a given pressure. To quantify this trend, we compute $d_{PP}(n) = \sqrt{(P^p(n) - P^l(n))^2}$. The metric $d_{PP}(n)$, reported in the inset, gives a measure of how different the topology of a plastic phase $P^p(n)$ is from that of the liquid phase $P^l(n)$. At 400 K, the topology of the plastic phase clearly deviates from that of the liquid with strongest deviations in correspondence of $n = 8$. Upon increasing the temperature, the entries of d_{PP} corresponding to shorter rings decrease in value (green diamonds and blue triangles), while those corresponding to longer rings remain mostly unaffected. The overall trend here presented is general and independent

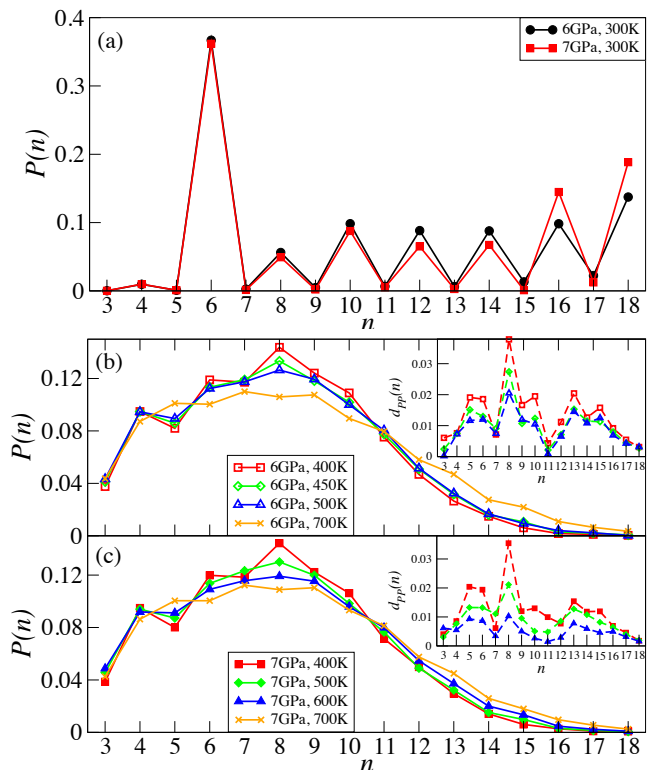


FIG. 2. Panel (a): ring distribution $P(n)$ computed for ice VII at 6 GPa and 300 K (black circles) and at 7 GPa and 300 K (red squares). Panel (b): $P(n)$ computed for plastic phases at 6 GPa and $T = 400, 450$ and 500 K as red, green and blue empty symbols, respectively, and for liquid phase at 6 GPa and $T = 700$ K as orange symbols. Panel (c): $P(n)$ computed for plastic phases at 7 GPa and $T = 400, 500$ and 600 K as red, green and blue filled symbols, respectively, and for liquid phase at 7 GPa and $T = 700$ K as orange symbols. Insets in panel a) and b): difference between $P(n)$ of the plastic phase and the $P(n)$ of the crystal phase for a given n .

on the pressure, and the case at $P = 7$ GPa is reported in fig. 2 (c) for comparison. A snapshot of the network in plastic ice VII is reported in fig. 3 b), where we emphasize an eleven-folded ring, absent in the network of ice VII.

Our study shows that the topology of the HBNs in plastic ice VII (as well as in high pressure liquid water) are more complex than that of water phases at lower pressures, where configurations with $n > 10$ are rarely populated^{58–60,85}. Considering that the topology of the HBN sets the properties of water^{58,60} and that ices with proton mobility are endowed with a spectrum of electrical conductivity^{32,35}, we posit that the complex HBN of plastic ice might play a yet unexplored important role in planetary science.

As we have previously stated, ice VII has two interpenetrating cubic lattices with two independent HBNs, which we will call network **A** and network **B**. In order to fully rationalize the nature of the HBN in plastic ice, it

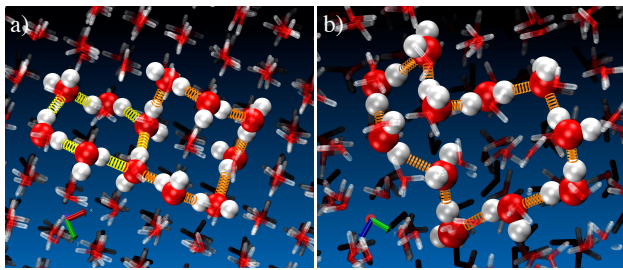


FIG. 3. Panel a): representative snapshot of the hydrogen bond network in ice VII. Oxygen atoms are depicted as red spheres, hydrogen atoms are white spheres. Two rings, namely a hexagonal ($n = 6$, yellow lines) and a octagonal ($n = 8$, orange lines) are emphasized to clarify the concept of ring. Panel b): representative snapshot of the hydrogen bond network in plastic ice VII. A eleven-folded ring (absent in the network of ice VII) is emphasized with orange lines.

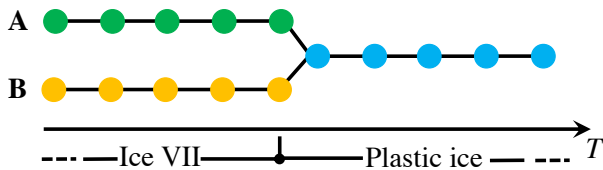


FIG. 4. Schematic representation of the evolution of networks **A** and **B** as a function of the applied temperature at a given pressure. The two networks are independent in ice VII and mix in the plastic phase. Each circle represent a state point. The mixing between the two networks occur in the timescale of molecular rotations.

is important to investigate whether molecular rotations mix the two networks, which therefore would intertwine and become dependent, or whether the two networks remain separate and independent. In order to address this issue, we have labeled each water molecule in ice VII belonging to the network **A** or to the network **B**. Switching on molecular rotations in the plastic phase, we have recorded the list of bonded neighbors for each molecule belonging to network **A** (**B**) and checked which network the neighbors belong to. We have found that the two networks indeed mix, hence indicating that the two independent HBNs characterizing ice VII, melt. The mixing between the two networks occurs on timescales comparable to the molecular rotations. In fig. 4 we report a pictorial representation of the temperature-dependence of the two networks **A** and **B**. The networks are independent in ice VII and the mixing occurring in the plastic phase is reported as a single line.

The activation of molecular rotations in the plastic phase has direct consequences on the amplitude of vibrations of oxygen atoms around their equilibrium positions. As shown in fig. 5, the amplitude of oxygen vibrations δr measured by the mean squared displacement in the plastic phase is almost four times larger compared to that of

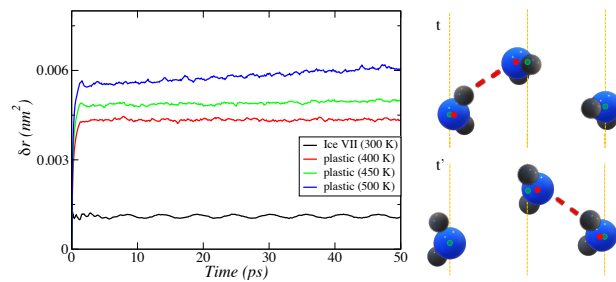


FIG. 5. Oscillation δr computed in terms of mean squared displacement on the isobar at 6 GPa. Ice VII is reported as black line, while the plastic phase at 400 K, 450 K and 500 K as red, green and blue lines, respectively. The right panel reports a pictorial representation of the oscillations of oxygen atoms around the equilibrium lattice point induced by the change of bonded molecules occurring from time t to time t' . The green dots represent the equilibrium positions, while the red dots the shifted positions induced by the formation of an HB emphasized as red dashed lines.

ice VII. In fig. 5 we report the values of δr at 6 GPa for ice VII at 300 K (black) and the plastic phase at 400 K (red), 450 K (green) and 500 K (blue). We can observe that the value of δr jumps from from $\sim 0.001 \text{ nm}^2$ in ice VII at 300 K (black) to $\sim 0.004 \text{ nm}^2$ in plastic ice VII at 400 K (red). Upon increasing the temperature, the increment in the value of δr is smaller compared to the jump observed entering the plastic phase. Therefore, we infer that the higher oscillations in the plastic phase with respect to ice VII are caused by molecular rotations: oxygen atoms are pulled in the direction of constantly changing hydrogen atoms resulting in enhanced deviations from the equilibrium position. A pictorial representation of such effect is reported in the right panel of fig. 5, where the vertical orange lines and the green dots indicate the equilibrium lattice positions and the red dots the displaced oxygen centers induced by the change of hydrogen bond occurring moving from time t to time t' .

In order to delve deeper into the properties of the HBN of plastic ice, we have inspected the percentage of broken and intact HBs, which provide information on the nature of the HBN and on the fluidity of water molecules^{66–68}. In fig. 6 we report the percentage n_d of having a coordination configuration of the kind $A_x D_y$ with x acceptors A and y donors D , for the case at $P = 6 \text{ GPa}$ in panel (a) and $P = 7 \text{ GPa}$ in panel (b), respectively. As expected, the HBN of ice VII is dominated by $A_2 D_2$ configurations, meaning that most of water molecules accept 2 HBs and donate 2 HBs. Increasing the temperature the percentage of $A_2 D_2$ drops drastically and other configurations increase, indicating that the HBN is populated by coordination defects. However, we can observe that plastic phases are characterized by different distributions depending on the temperature, hence confirming that the HBN of plastic ice is affected by the thermodynamic conditions. For a given pressure, the plastic phases

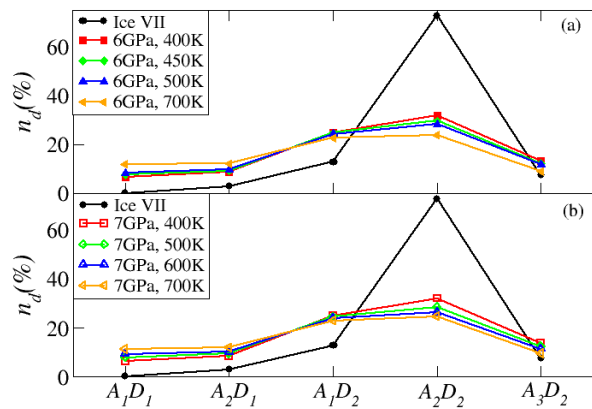


FIG. 6. Percentage n_d of having a coordination configurations of the kind $A_x D_y$, with x acceptors A and y donors D . Panel (a): n_d for ice VII (black filled circles) and for the isobar at $P = 6$ GPa (filled symbols). Panel (b): n_d for ice VII (black filled circles) and for the isobar at $P = 7$ GPa (empty symbols).

at increasingly high temperatures represent intermediate phases between ice VII and the liquid phase.

IV. CONCLUSIONS

Plastic ice VII sits at the boundaries of crystalline ice VII and liquid water at thermodynamic conditions of relevance for planetary investigations, where the flux of hydrogen atoms seems to play a crucial role in defining the properties of water-rich planets, and the transfer of salts from the core to liquid oceans may promote chemical reactions important to sustain life. Therefore, in this study we have assessed the properties of the dynamical hydrogen bond network (HBN) in plastic ice VII modeled via classical molecular dynamics simulations on a wide range of thermodynamic conditions. We have observed that the topology of the HBN of plastic ice carries some degree of reminiscence of the crystal ice VII, stronger at thermodynamic conditions proximal to ice VII, and gradually lessening upon approaching the liquid state.

Although ice VII is composed by two interpenetrating and independent cubic lattices, molecular rotations allow the two networks to "melt" and mix becoming indistinguishable in the plastic phase. Nonetheless, molecular rotations induce enhanced fluctuations of the oxygen atoms around their equilibrium lattice positions.

Planetary science has so far focused on liquid water, crystalline and superionic ices to explain the properties of water-rich planets. We propose that the dynamical, complex HBN of plastic ices (shall their existence be confirmed experimentally) makes them potential candidate to play an active role in the geology of planets and in the transfer of salt from their cores to liquid oceans. Finally, our results expand our understanding of the properties

at high pressures.

ACKNOWLEDGMENTS

This work used supercomputing facilities provided by the STFC-Hartree Centre. JR acknowledges support from the European Research Council Grant No. DLV-759187.

- ¹C. G. Salzmann. Advances in the experimental exploration of water's phase diagram. *J. Chem. Phys.*, 150:060901, 2019.
- ²F. Martelli. *Properties of Water from Numerical and Experimental Perspectives*. CRC Press, 2022.
- ³W. J. Nellis, D. C. Hamilton, N. C. Holmes, H. B. Radousky, F. H. Ree, A. C. Mitchell, and M. Nicol. The nature of the interior of uranus based on studies of planetary ices at high dynamic pressure. *Science*, 240:779, 1988.
- ⁴R. L. Kirk and D. J. Stevenson. Hydromagnetic constraints on deep zonal flow in the giant planets. *Astrophys. J.*, 316:836, 1988.
- ⁵R. Redmer, T. R. Mattsson, N. Nettelmann, and M. French. The phase diagram of water and the magnetic fields of uranus and neptune. *Icarus*, 211:798–803, 2011.
- ⁶L. E. Bove, S. Klotz, T. Strässle, M. Koza, J. Teixeira, and A. M. Saitta. Translational and rotational diffusion in water in the gigapascal range. *Phys. Rev. Lett.*, 111:185901, 2013.
- ⁷J. Sun, B. K. Clark, S. Torquato, and R. Car. The phase diagram of high-pressure superionic ice. *Nat. Comm.*, 6:8156, 2015.
- ⁸O. Tschaurer, S. Huang, E. Greenberg, V. B. Prakapenja, C. Ma, G. R. Rossman, A. H. Shen, D. Zhang, M. Newville, A. Lanzirrotti, and J. Tait. Ice-vii inclusions in diamonds: Evidence for aqueous fluid in earth's deep mantle. *Science*, 359:1136–1139, 2018.
- ⁹R.-S. Taubner, K. Olsson-Francis, S. D. Vance, N. K. Ramkissoon, F. Postberg, J.-P. de Vera, A. Antunes, E. Camprubi Casas, Y. Sekine, L. Noack, L. Barge, J. Goodman, M. Jebbar, B. Journaux, Ö. Karatekin, F. Klenner, E. Rabbow, P. Retberg, T. Rückriemen-Bez, J. Saur, T. Shibuya, and K. M. Soderlund. Experimental and simulation efforts in the astrobiological exploration of exooceans. *Space Sci. Rev.*, 216:9–41, 2020.
- ¹⁰F. Martelli, N. Giovambattista, S. Torquato, and R. Car. Searching for crystal-ice domains in amorphous ices. *Phys. Rev. Materials*, 2:075601, 2018.
- ¹¹F. Martelli, S. Torquato, N. Giovambattista, and R. Car. Large-scale structure and hyperuniformity of amorphous ices. *Phys. Rev. Lett.*, 119:136002, 2017.
- ¹²F. Martelli, F. Leoni, F. Sciortino, and J. Russo. Connection between liquid and non-crystalline solid phases of water. *J. Chem. Phys.*, 153:104503, 2020.
- ¹³J. Russo, F. Leoni, F. Martelli, and F. Sciortino. The physics of empty liquids: from patchy particles to water. *Rep. Prog. Phys.*, 85:016601, 2022.
- ¹⁴C. M. Tonaier, E.-M. Köck, T. M. Gasser, V. Fuentes-Landete, R. Henn, S. Mayr, C. G. Kirchler, C. W. Huck, and T. Loerting. Near-infrared spectra of high-density crystalline h₂o ices ii, iv, v, vi, ix, and xii. *J. Phys. Chem. A*, 125:1062–1068, 2021.
- ¹⁵L. Tian, A. I. Kolesnikov, and J. Li. Ab initio simulation of hydrogen bonding in ices under ultra-high pressure. *J. Chem. Phys.*, 137:204507, 2012.
- ¹⁶M. Millot, F. Coppari, J. R. Rygg, A. Correa Barrios, S. Hamel, D. C. Swift, and J. H. Eggert. Nanosecond x-ray diffraction of shock-compressed superionic water ice. *Nature*, 569:251–255, 2019.
- ¹⁷C. G. Salzmann, P. G. Radaelli, B. Slater, and J. L. Finney. The polymorphism of ice: five unresolved questions. *Phys. Chem. Chem. Phys.*, 13:18468–18480, 2011.
- ¹⁸C. G. Salzmann, P. G. Radaelli, A. Hallbrucker, E. Mayer, and J. L. Finney. The preparation and structures of hydrogen ordered phases of ice. *Science*, 311:1758–1761, 2006.
- ¹⁹C. G. Salzmann, P. G. Radaelli, E. Mayer, and J. L. Finney. Ice xv: A new thermodynamically stable phase of ice. *Phys. Rev. Lett.*, 103:105701, 2009.
- ²⁰S. Klotz, L. E. Bove, T. Strässle, T. C. Hansen, and A. M. Saitta. The preparation and structure of salty ice vii under pressure. *Nat. Mater.*, 8:405–409, 2009.

- ²¹S. Klotz, K. Komatsu, F. Pietrucci, H. Kagi, A.-A. Ludl, S. Machida, T. Hattori, A. Sano-Furukawa, and L. E. Bove. Ice vii from aqueous salt solutions: From a glass to a crystal with broken h-bonds. *Sci. Rep.*, 632040:32040, 2016.
- ²²B. J. Murray, T. L. Malkin, and C. G. Salzmann. The crystal structure of ice under mesospheric conditions. *J. Atmospheric Sol.-Terr. Phys.*, 127:78–82, 2015.
- ²³J. D. Bernal and R. H. Fowler. A theory of water and ionic solution, with particular reference to hydrogen and hydroxyl ions. *J. Chem. Phys.*, 1:515–548, 1933.
- ²⁴C. P. Herrero and R. Ramírez. Topological characterization of crystalline ice structures from coordination sequences. *Phys. Chem. Chem. Phys.*, 15:16676–16685, 2013.
- ²⁵M. Song, H. Yamawaki, H. Fujihisa, M. Sakashita, and K. Aoki. Infrared investigation on ice viii and the phase diagram of dense ices. *Phys. Rev. B*, 68:014106, 2003.
- ²⁶M. Song, H. Yamawaki, H. Fujihisa, M. Sakashita, and K. Aoki. Infrared observation of the phase transitions of ice at low temperatures and pressures up to 50 gpa and the metastability of low-temperature ice vii. *Phys. Rev. B*, 68:024108, 2003.
- ²⁷A. N. Dunaeva, D. V. Antsyshkin, and O. L. Kuskov. Phase diagram of h₂o: Thermodynamic functions of the phase transitions of high-pressure ices. *Sol. Syst. Res.*, 44:202–222, 2010.
- ²⁸L. E. Bove, R. Gaal, Z. Raza, A.-A. Ludl, S. Klotz, A. M. Saitta, A. F. Goncharov, and P. Gillet. Effect of salt on the h-bond symmetrization in ice. *Proc. Natl. Acad. Sci. USA*, 112:8216–8220, 2015.
- ²⁹B. Journaux, I. Daniel, S. Petitgirard, H. Cardon, J.-P. Perrillat, R. Caracas, and M. Mezouar. Salt partitioning between water and high-pressure ices. implication for the dynamics and habitability of icy moons and water-rich planetary bodies. *Earth Planet. Sci. Lett.*, 463:36–47, 2017.
- ³⁰J.-A. Hernandez, R. Caracas, and S. Labrosse. Stability of high-temperature salty ice suggests electrolyte permeability in water-rich exoplanet icy mantles. *Nat. Commun.*, 13:3303, 2022.
- ³¹Z. Futera, J. S. Tse, and N. J. English. Possibility of realizing superionic ice vii in external electric fields of planetary bodies. *Sci. Adv.*, 6:eaa2915, 2020.
- ³²C. Cavezzoni, G. L. Chiarotti, S. Scandolo, E. Tosatti, M. Bernasconi, and M. Parrinello. Superionic and metallic states of water and ammonia at giant planet conditions. *Science*, 283:44–46, 1999.
- ³³C. P. Herrero and R. Ramírez. Path-integral simulation of ice vii: Pressure and temperature effects. *Chem. Phys.*, 461:125–136, 2015.
- ³⁴V. B. Prakapenka, N. Holtgrewe, S. S. Lobanov, and A. F. Goncharov. Structure and properties of two superionic ice phases. *Nat. Phys.*, 17:1233–1238, 2021.
- ³⁵J.-A. Hernandez and R. Caracas. Superionic-superionic phase transitions in body-centered cubic h₂o ice. *Phys. Rev. Lett.*, 117:135503, 2016.
- ³⁶M. French, M. Desjarlous, and M. P. Redmer. Ab initio calculation of thermodynamic potentials and entropies for superionic water. *Phys. Rev. E*, 93:022140, 2016.
- ³⁷J.-A. Hernandez and B. Caracas. Proton dynamics and the phase diagram of dense water ice. *J. Chem. Phys.*, 148:214501, 2018.
- ³⁸Y. Takii, K. Koga, and H. Tanaka. A plastic phase of water from computer simulation. *J. Chem. Phys.*, 128:204501, 2008.
- ³⁹J. L. Aragonés and C. Vega. Plastic crystal phases of simple water models. *J. Chem. Phys.*, 130:244504, 2009.
- ⁴⁰J. L. Aragonés, M. M. Conde, E. G. Noya, and C. Vega. The phase diagram of water at high pressures as obtained by computer simulations of the tip4p/2005 model: the appearance of a plastic crystal phase. *Phys. Chem. Chem. Phys.*, 11:543–555, 2009.
- ⁴¹K. Mochizuki, K. Himoto, and M. Matsumoto. Diversity of transition pathways in the course of crystallization into ice vii. *Phys. Chem. Chem. Phys.*, 16:16419, 2014.
- ⁴²I. Skarmoutsos, S. Mossa, and E. Guardia. The effect of polymorphism on the structural, dynamic and dielectric properties of plastic crystal water: A molecular dynamics simulation perspective. *J. Chem. Phys.*, 150:124506, 2019.
- ⁴³Y. Adachi and K. Koga. Structure and phase behavior of high-density ice from molecular-dynamics simulations with the reaxff potential. *J. Chem. Phys.*, 153:114501, 2020.
- ⁴⁴J. T. Yoon, L. A. Patel, T. Ju, M. J. Vigil, A. T. Findikoglu, R. P. Currier, and K. A. T. Maerzke. Thermodynamics, dynamics, and structure of supercritical water at extreme conditions. *Phys. Chem. Chem. Phys.*, 22:16051–16062, 2020.
- ⁴⁵A. Henao, J. M. Salazar-Rios, and E. Guardia L. C. Pardo. Structure and dynamics of water plastic crystals from computer simulations. *J. Chem. Phys.*, 154:104501, 2021.
- ⁴⁶I. Skarmoutsos, A. Henao, E. Guardia, and J. Samios. On the different faces of the supercritical phase of water at a near-critical temperature: Pressure-induced structural transitions ranging from a gaslike fluid to a plastic crystal polymorph. *J. Phys. Chem. B*, 125:10260–10272, 2021.
- ⁴⁷D. Prasad and N. Mitra. High-temperature and high-pressure plastic phase of ice at the boundary of liquid water and ice vii. *Proc. R. Soc. A*, 478:20210958, 2022.
- ⁴⁸M. Matsumoto, K. Himoto, and H. Tanaka. Spin-one ising model for ice vii–plastic ice phase transitions. *J. Phys. Chem. B*, 118:13387–13392, 2014.
- ⁴⁹J. L. F. Abascal and C. Vega. A general purpose model for the condensed phases of water: Tip4p/2005. *J. Chem. Phys.*, 123:234505, 2005.
- ⁵⁰M. M. Conde, M. A. Gonzalez, J. L. F. Abascal, and C. Vega. Determining the phase diagram of water from direct coexistence simulations: The phase diagram of the tip4p/2005 model revisited. *J. Chem. Phys.*, 139:154505, 2013.
- ⁵¹M. J. Abraham, T. Murtola, R. Schulz, S. Páll, J. C. Smith, B. Hess, and E. Lindahl. Gromacs: High performance molecular simulations through multi-level parallelism from laptops to supercomputers. *SoftwareX*, 1:19–25, 2015.
- ⁵²S. Nosé. A molecular dynamics method for simulations in the canonical ensemble. *Mol. Phys.*, 52:255–268, 1984.
- ⁵³W. G. Hoover. Canonical dynamics: Equilibrium phase-space distributions. *Phys. Rev. A*, 31:1695, 1985.
- ⁵⁴M. Parrinello and A. Rahman. Polymorphic transitions in single crystals: A new molecular dynamics method. *J. Appl. Phys.*, 52:7182, 1981.
- ⁵⁵W. C. Swope, H. C. Andersen, P. H. Berens, and K. R. Wilson. A computer simulation method for the calculation of equilibrium constants for the formation of physical clusters of molecules: Application to small water clusters. *J. Chem. Phys.*, 76:637–649, 1982.
- ⁵⁶M. Matsumoto, T. Yagasaki, and H. Tanaka. Genice: Hydrogen-disordered ice generator. *J. Comp. Chem.*, 39:61–64, 2017.
- ⁵⁷F. Martelli. Steady-like topology of the dynamical hydrogen bond network in supercooled water. *PNAS Nexus*, 2022. doi:10.1093/pnasnexus/pgac090.
- ⁵⁸F. Martelli. Topology and complexity of the hydrogen bond network in classical models of water. *J. Mol. Liq.*, 329:115530, 2021.
- ⁵⁹M. Formanek and F. Martelli. Probing the network topology in network-forming materials: The case of water. *AIP Adv.*, 10:055205, 2020.
- ⁶⁰F. Martelli. Unravelling the contribution of local structures to the anomalies of water: The synergistic action of several factors. *J. Chem. Phys.*, 150:094506, 2020.
- ⁶¹G. Camisasca, D. Schlesinger, I. Zhovtobriukh, G. Pitsevich, and L. G. M. Pettersson. A proposal for the structure of high- and low-density fluctuations in liquid water. *J. Chem. Phys.*, 151:034508, 2019.
- ⁶²J. C. Palmer, F. Martelli, Y. Liu, R. Car, A. Z. Panagiotopoulos, and P. G. Debenedetti. Metastable liquid–liquid transition in a molecular model of water. *Nature*, 510:385–388, 2014.
- ⁶³B. Santra, R. A. DiStasio Jr., F. Martelli, and R. Car. *Mol. Phys.*, 113:2829–2841, 2015.
- ⁶⁴J. Castagna, F. Martelli, K. E. Jordan, and J. Crain. Simulation of large molecular systems with electronically-derived forces. *Comp. Phys. Comm.*, 264:107959, 2021.
- ⁶⁵R. Foffi, J. Russo, and F. Sciortino. Structural and topological changes across the liquid–liquid transition in water. *J. Chem. Phys.*, 154:184506, 2021.
- ⁶⁶F. Martelli, J. Crain, and G. Franzese. Network topology in water nanoconfined between phospholipid membranes. *ACS Nano*, 14:8616–8623, 2020.
- ⁶⁷M. Chiricotto, F. Martelli, G. Giunta, and P. Carbone. The role of long-range electrostatic interactions and local topology of the hydrogen bond network in the wettability of fully and partially wetted single and multilayer graphene. *J. Phys. Chem. C*, 125:6367–6377, 2021.
- ⁶⁸Z. Wei, Chiricotto M, J. D. Elliott, F. Martelli, and P. Carbone. Wettability of graphite under 2d confinement. *Carbon*, 198:132–141, 2022.
- ⁶⁹I. Bakó, J. Oláh, A. Lábás, S. Bálint, L. Pusztai, and M. C. Bellissent Funel. Water-formamide mixtures: Topology of the hydrogen-bonded network. *J. Mol. Liq.*, 228:25–31, 2017.

- ⁷⁰S. Pothoczki, L. Pusztai, and I. Bakó. Variations of the hydrogen bonding and hydrogen-bonded network in ethanol–water mixtures on cooling. *J. Phys. Chem. B*, 122:6790–6800, 2018.
- ⁷¹S. Pothoczki, L. Pusztai, and I. Bakó. Molecular dynamics simulation studies of the temperature-dependent structure and dynamics of isopropanol–water liquid mixtures at low alcohol content. *J. Phys. Chem. B*, 123:7599–7610, 2019.
- ⁷²L. Li, J. Zhong, Y. Yan, J. Zhang, J. Xu, J. S. Francisco, and X. C. Zeng. Unraveling nucleation pathway in methaneclathrate formation. *Proc. Natl. Acad. Sci. USA*, 117:24701–24708, 2020.
- ⁷³S. Le Roux and P. Jund. Ring statistics analysis of topological networks: New approach and application to amorphous ges_2 and sio_2 systems. *Comp. Mater. Sci.*, 49:70–83, 2010.
- ⁷⁴X. Yuan and A. N. Cormack. Efficient algorithm for primitive ring statistics in topological networks. *Comp. Mater. Sci.*, 24:343–360, 2002.
- ⁷⁵G. Opetal, T. C. Petersen, I. K. Snook, and D. G. McCulloch. Modeling of structure and porosity in amorphous silicon systems using monte carlo methods. *J. Chem. Phys.*, 126:214705, 2007.
- ⁷⁶P. Kumar Roy, M. Heyde, and A. Heuer. Modelling the atomic arrangement of amorphous 2d silica: a network analysis. *Phys. Chem. Chem. Phys.*, 20:14725–14739, 2018.
- ⁷⁷P. Kumar Roy and A. Heuer. Ring statistics in 2d silica: Effective temperatures in equilibrium. *Phys. Rev. Lett.*, 122:016104, 2019.
- ⁷⁸D. K. Limbu, R. Atta-Fynn, and P. Biswas. Atomistic simulation of nearly defect-free models of amorphous silicon: An information-based approach. *MRS Advances*, 4:87–93, 2019.
- ⁷⁹J. Hagedüs and S. R. Elliott. Microscopic origin of the fast crystallization ability of ge–sb–te phase-change memory materials. *Nat. Mater.*, 7:399–405, 2008.
- ⁸⁰W.-X. Song, F. Martelli, and Z. Song. Observing the spontaneous formation of a sub-critical nucleus in a phase-change amorphous material from ab initio molecular dynamics. *Mater. Sci. Semicond.*, 136:106102, 2021.
- ⁸¹A. Neophytou, D. Chakrabarti, and F. Sciortino. Facile self-assembly of colloidal diamond from tetrahedral patchy particles via ring selection. *Proc. Natl. Acad. Sci. USA*, 118:e2109776118, 2021.
- ⁸²A. Luzar and D. Chandler. Hydrogen-bond kinetics in liquid water. *Nature*, 379:55–57, 1996.
- ⁸³D. Prada-Gracia, R. Shevchuk, and F. Rao. The quest for self-consistency in hydrogen bond definitions. *J. Chem. Phys.*, 139:084501, 2013.
- ⁸⁴R. Shi, J. Russo, and H. Tanaka. Common microscopic structural origin for water’s thermodynamic and dynamic anomalies. *J. Chem. Phys.*, 149:224502, 2018.
- ⁸⁵F. Martelli, H.-Y. Ko, E. C. Oğuz, and R. Car. Local-order metric for condensed phase environments. *Phys. Rev. B*, 97:064105, 2016.

